Electronic Supplementary Material (ESI) for Nanoscale.

Supplementary Information

Solvatochromism in SWCNTs Suspended by Conjugated Polymers in Organic Solvents

Andrzej Dzienia[1,2,*], Dominik Just[1], Dawid Janas[1,*]

[1] *Department of Chemistry, Silesian University of Technology, B. Krzywoustego 4, 44-100, Gliwice, Poland*

[2] *Institute of Materials Engineering, University of Silesia in Katowice, Bankowa 12, 40-007 Katowice, Poland*

*Corresponding authors: Andrzej.Dzienia@polsl.pl (A.D.), Dawid.Janas@polsl.pl (D.J.)

Table of Contents

1. Materials 3

1.1. Reagents for polymer synthesis 3

1.2. Solvents 3

1.3. Carbon nanotubes 4

2. Characterization 5

2.1. Nuclear Magnetic Resonance (^{1}H NMR) 5

2.2. Size Exclusion Chromatography (SEC) 5

2.3. Polymer synthesis and characterization 5

3. Optical transitions of specific SWCNTs in water and organic solvents 9

4. Characterization of the raw material 10

5. Influence of polymer:SWCNT ratios on the composition of the supernatant 11

6. Deconvolution of the composition of the supernatants obtained using non-selective and selective polymers 12

7. Deconvolution of the composition of the supernatants obtained using non-selective and selective polymers 13

8. Gauging the solvatochromic effect using SWCNTs isolated with selective polymers 14

9. Attempts to correlate properties of the solvent with optical characteristics of various SWCNTs separated in it 17

10. References 21

1. Materials

All chemical reagents and solvents were used as supplied, without additional purification or drying (except when stated otherwise). The purity of the reagents, along with the manufacturer and data allowing identification, can be found below.

1.1. Reagents for polymer synthesis

9,9-dioctylfluorene-2,7-bis(boronic acid pinacol ester) (Angene, cat. number: AG0034EZ, CAS: 196207-58-6, purity: 98%), 2,5-dibromothiophene (AmBeed, cat. number: A137367-10g, CAS: 3141-27-3, purity: 98%), 2,7-Dibromo-9,9-dioctyl-9H-fluorene (Sigma Aldrich, cat. number: 560073-25g, CAS: 198964-46-4, purity: 96%), 6,6'-Dibromo-2,2'-bipyridyl (TCL, cat. number: D3988-5G, purity: >95%), Aliquat 336 TG (Alfa Aesar, cat. number: A17247, CAS: 63393-96-4, purity: N/A), tetrakis(triphenylphosphine)palladium, $Pd(PPh_3)_4$, (Apollo Scientific, cat. number: OR4225, CAS: 14221-01-3, purity: >99%).

1.2. Solvents

Toluene (Alfa Aesar, cat. number: 19376.K2, CAS: 108-88-3, spectrophotometric grade, purity: >99.7%), tetrahydronaphthalene (tetralin, Fisher Chemical, cat. number: T/0850/08, CAS: 119-64-2, purity: >97%,), m-xylene (Alfa Aesar, cat. number: L03788.AP, CAS: 108-38-3, purity: 99%), o-xylene (Alfa Aesar, cat. number: A11358.AP, CAS: 95-47-6, purity: 99%), anisole (Alfa Aesar, cat. number: A12997.36, CAS: 100-66-3, purity: 99%), tetrahydrofuran (Alfa Aesar, cat. number: L13304.AP, CAS: 109-99-9, purity: 99%), benzene (Roth, cat. number: ROTH-7173.3, CAS: 71-43-2, purity: 99.5%).

Table S1. Selected physicochemical parameters of applied solvents sorted in ascending order of density [1–9].

Solvent	Density [g/mL]	Viscosity at 20°C [mPa·s]	Polarity	Dielectric constant ε [F/m]	Dipole moment [D]	Refractive index η	Induction polarity function $f(\eta^2)$	Orientation polarity function $f(\varepsilon) - f(\eta^2)$
Benzene	0.876	0.65	0.111	2.28	0	0.005	1.501	0.455
Toluene	0.867	0.59	0.099	2.376	0.31	0.026	1.497	0.453
m-xylene	0.868	0.62	N/A	2.367	0.31	0.024	1.497	0.453
o-xylene	0.879	0.81	N/A	2.568	0.45	0.053	1.505	0.458
Tetralin	0.974	2.2	0.086	2.77	0	0.063	1.541	0.478
Anisole	0.995	0.98	0.198	4.3	1.4	0.222	1.518	0.465
THF	0.888	0.48	0.207	7.6	1.75	0.420	1.407	0.395
DMF	0.945	0.79	0.404	36.7	3.8	0.549	1.431	0.411

1.3. Carbon nanotubes

The study was carried out using (6,5)-enriched CoMoCAT SWCNTs (Sigma Aldrich, product number: 773735, lot: MKCM5514, purity: 95%-carbon basis) and HiPco nanotubes (NanoIntegris, lot: HP30-006).

2. Characterization

2.1. Nuclear Magnetic Resonance (^{1}H NMR)

Proton nuclear magnetic resonance (^{1}H NMR) spectra of polymers were recorded using a Varian Unity Inova spectrometer operating at 400 MHz with $CDCl_3$ as a solvent. ^{1}H-chemical shifts were measured in δ (ppm), using the chloroform-d residual peak, set at δ 7.26, as reference. Standard experimental conditions were used. NMR spectra of the synthesized polymers generated from the Bruker program are provided in the SI (Figs. S1-S3).

2.2. Size Exclusion Chromatography (SEC)

Molecular weights and dispersity (Đ) indices were determined using a size exclusion chromatography instrument (SEC, Agilent 1260 Infinity) (Agilent Technologies) equipped with an isocratic pump, autosampler, degasser, a thermostatic box for columns, and a differential refractometer MDS RI Detector. Addon Rev. B.01.02 data analysis software (Agilent Technologies) was used for data collection and processing. The SEC-calculated molecular weight was based on a calibration using linear polystyrene standards (580–300,000 g/mol). A pre-column guard, 5 µm 50 × 7.5 mm, and two columns, PLgel 5 µm MIXED-C 300 × 7.5 mm and PLgel 5 µm MIXED-D 300 × 7.5 mm, were used for separation. The measurements were obtained using $CHCl_3$ (HPLC grade) as the solvent at 30°C at a flow rate of 0.8 mL/min.

2.3. Polymer synthesis and characterization

Boronic ester (9,9-di-n-octylfluorene-2,7-diboronic acid bis(pinacol)ester, purity: 98%) (0.5 g, 0.763 mmol, 1 eq.) and the appropriate amount of dibromo derivative (2,5-dibromothiophene purity: 97%) (0.2243 g, 0.763 mmol, 1 eq.) were added to a high-pressure glass reactor vessel. The reactor was then filled with 1M Na_2CO_3 solution (12 ml) and toluene (12 ml). Finally, two drops of Aliquat 336 phase transfer catalyst (PTC) were added. The mixture was flushed with argon for 30 min, and subsequently $Pd(PPh_3)_4$ (0.026g, 0.023 mmol, 0.03 eq.) was added. The reaction mixture was then stirred vigorously at 85°C for 3 days. Subsequently, the reaction

mixture was cooled down, diluted with 200 ml of chloroform, and washed three times with 150 ml of water. The organic layer was collected and dried over $MgSO_4$, which was then removed by filtration. The collected material was evaporated to dryness and dissolved in a sufficient volume of chloroform (to give a low-viscosity liquid yielding small particles or thin fibers during precipitation). The final product was precipitated from a mixture of methanol and water (9:1). The fibrous polymer was collected by filtration, washed twice with 50 ml of cold methanol, and then twice with 50 ml of cold acetone.

Table S2. Macromolecular parameters of conjugated polymers synthesized for the study

Polymer	**Batch**	**M_n** [kg/mol]	**M_w** [kg/mol]	**Đ**
PFO-T	Low Mw	3200	4200	1.3
	High Mw	3950	7150	1.8
PFO	-	13000	41000	3.2
PFO-BPy	-	4700	7000	1.5

Analogously, PFO and PFO-BPy were prepared and used for selective extraction of (7,5) and (6,5) SWCNTs. NMR spectra of these compounds, which confirm their successful syntheses, are shown below in Fig. S1-S3.

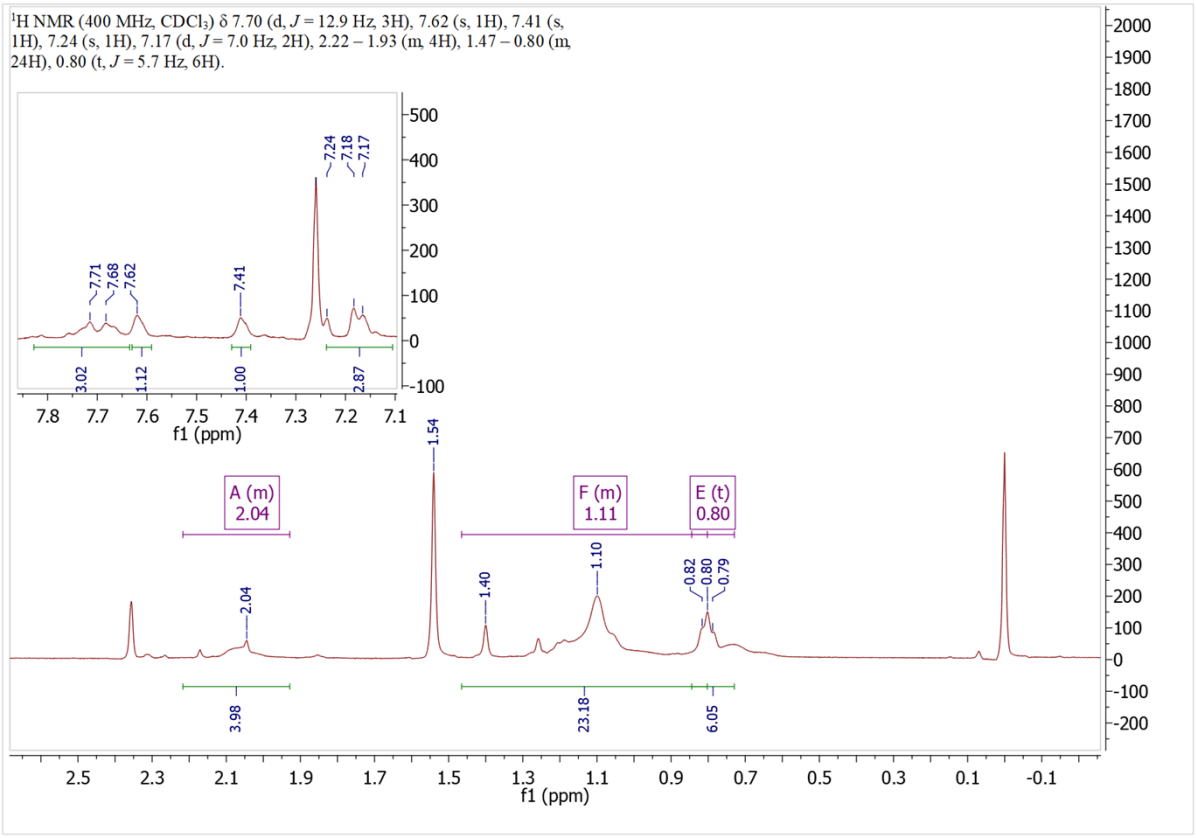

Figure S1. [1]H NMR spectrum of typical PFO-T synthesized in-house.

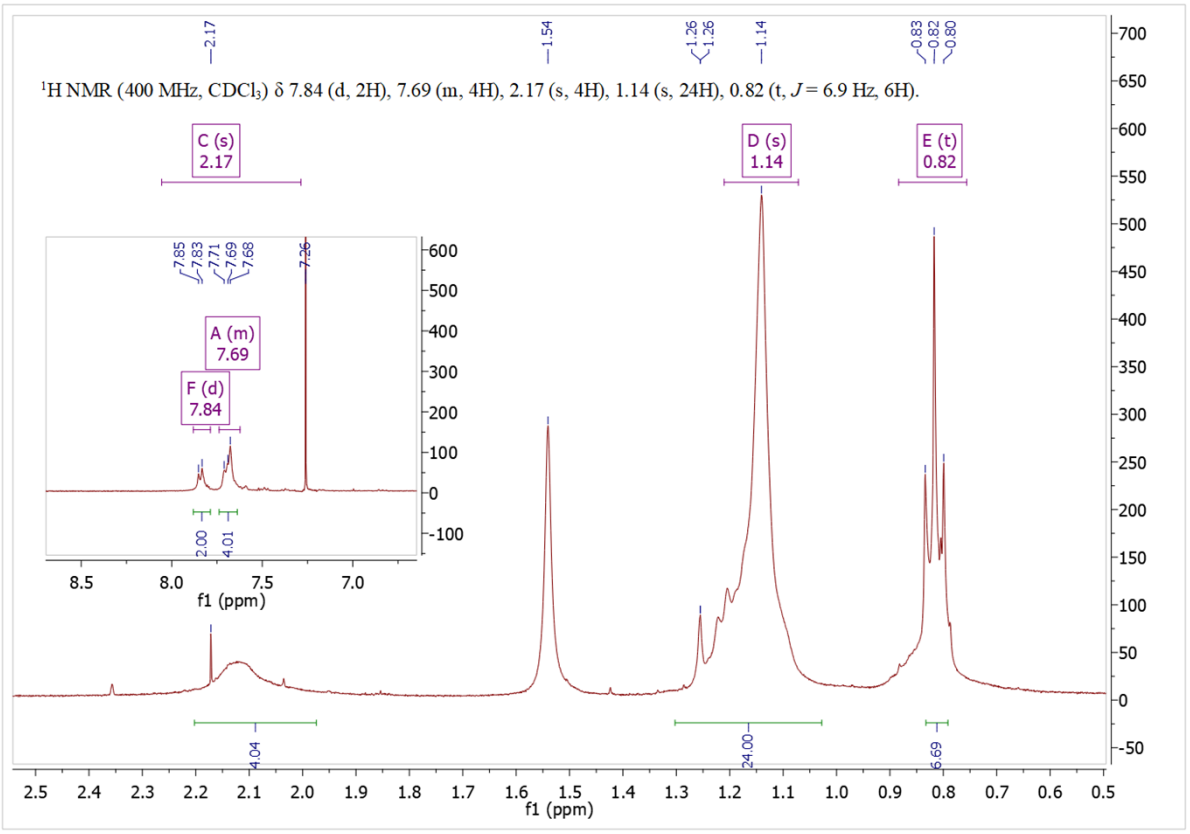

Figure S2. [1]H NMR spectrum of PFO synthesized in-house.

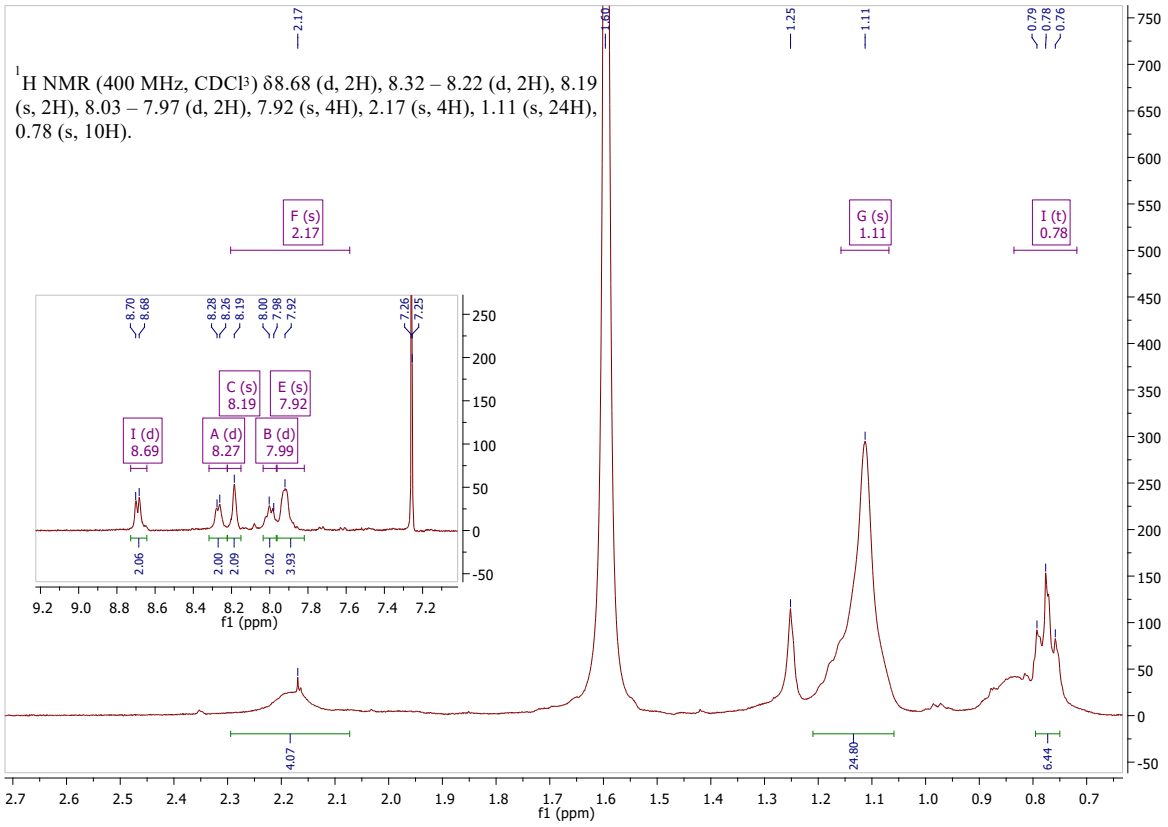

Figure S3. [1]H NMR spectrum of PFO-BPy synthesized in-house.

3. Optical transitions of specific SWCNTs in water and organic solvents

Table S3. Position of E_{11} peak maximum [nm] extracted from Figure 2.

Chirality	Solvent	Position of E_{11} peak maximum [nm]		
		Lowest value	Median value	Highest value
(6,5)	Aqueous	975	981	995
	Organic	970	992	1001
(7,3)	Aqueous	992	999	1009
	Organic	996	996	996
(7,5)	Aqueous	1022	1030	1044
	Organic	1016	1042	1070
(7,6)	Aqueous	1120	1128	1147
	Organic	1113	1140	1162
(8,1)	Aqueous	1039	1042	1046
	Organic	1060	1060	1060
(8,3)	Aqueous	952	959	973
	Organic	943	967	984
(8,4)	Aqueous	1111	1122	1140
	Organic	1106	1133	1160
(8,6)	Aqueous	1172	1181	1200
	Organic	1166	1194	1213
(8,7)	Aqueous	1265	1279	1295
	Organic	1260	1288	1316
(9,1)	Aqueous	912	917	926
	Organic	923	923	923
(9,2)	Aqueous	1138	1149	1166
	Organic	1159	1159	1160
(9,4)	Aqueous	1100	1109	1130
	Organic	1097	1122	1144
(9,5)	Aqueous	1241	1249	1257
	Organic	1239	1269	1301
(9,7)	Aqueous	1322	1332	1345
	Organic	1320	1344	1368
(10,2)	Aqueous	1053	1061	1077
	Organic	1047	1072	1085
(10,3)	Aqueous	1249	1257	1274
	Organic	1244	1276	1316
(10,5)	Aqueous	1249	1257	1269
	Organic	1249	1272	1301
(10,6)	Aqueous	1377	1390	1425
	Organic	1377	1408	1440
(11,3)	Aqueous	1197	1206	1229
	Organic	1197	1215	1229
(11,4)	Aqueous	1356	1378	1392
	Organic	1371	1388	1407

4. Characterization of the raw material

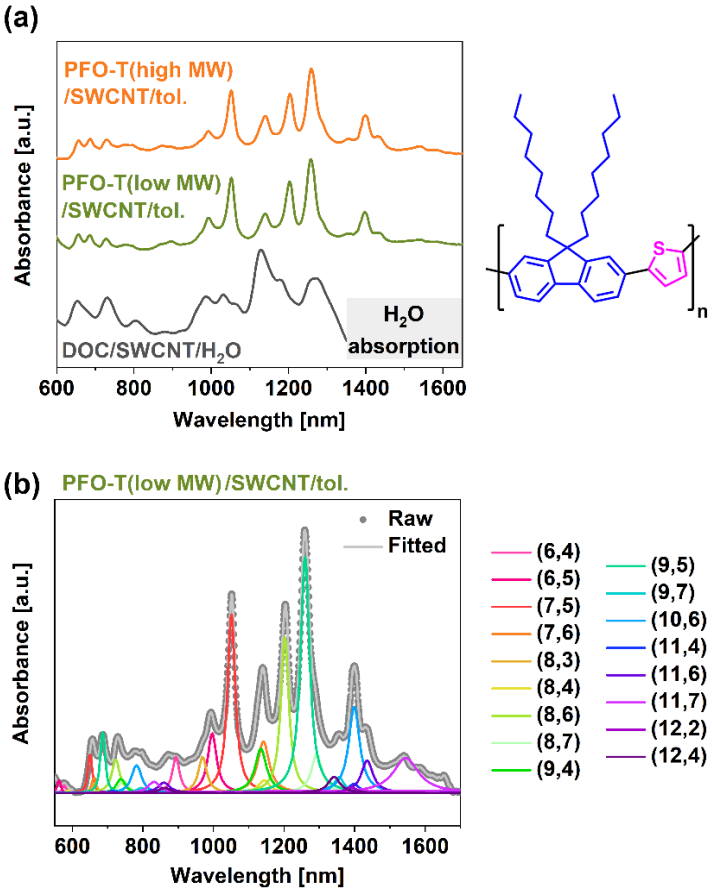

Figure S4 (a) Offset absorption spectra of SWCNTs individualized in water by sodium deoxycholate and toluene by PFO-T (shown on the right) of low and high molecular weight (6:1 ratio of polymer:SWCNTs by weight). (b) The deconvoluted absorption spectrum of SWCNTs suspended by PFO-T of low molecular weight in toluene.

Deconvolution of the data was conducted using the PTF Fit application [10]. First, baseline modeled using the function devised by Nair et al. [11] was subtracted from raw data and then the individual peaks were resolved using the Voigt function. The position of maxima of these peaks was used for the determination of solvatochromic shifts, whereas the area of the peaks enabled estimation of the concentrations of specific SWCNT chiralities.

5. Influence of polymer:SWCNT ratios on the composition of the supernatant

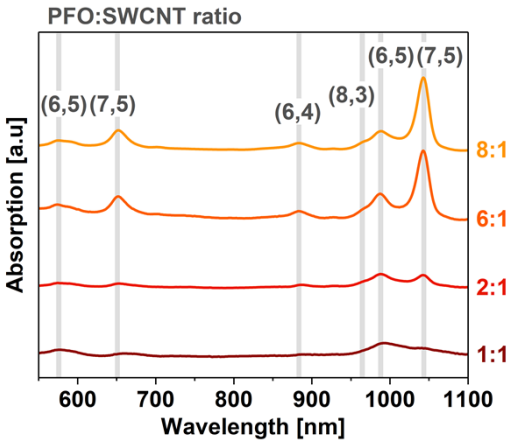

Figure S5. The impact of PFO:SWCNT ratio on the CPE separation.

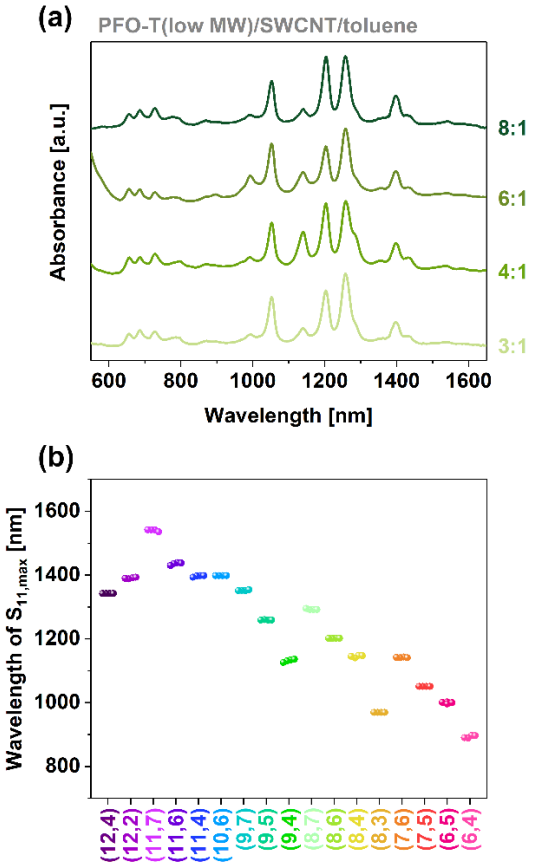

Figure S6 (a) Offset absorption spectra of SWCNTs individualized in toluene by PFO-T of low molecular weight at specified ratios of polymer to SWCNTs by weight. (b) Peak maxima of S_{11} transitions of SWCNTs of indicated chiralities measured for different polymer:SWCNT ratios (shown with the ascending polymer:SWCNT ratio from left to right).

6. Deconvolution of the composition of the supernatants obtained using non-selective and selective polymers

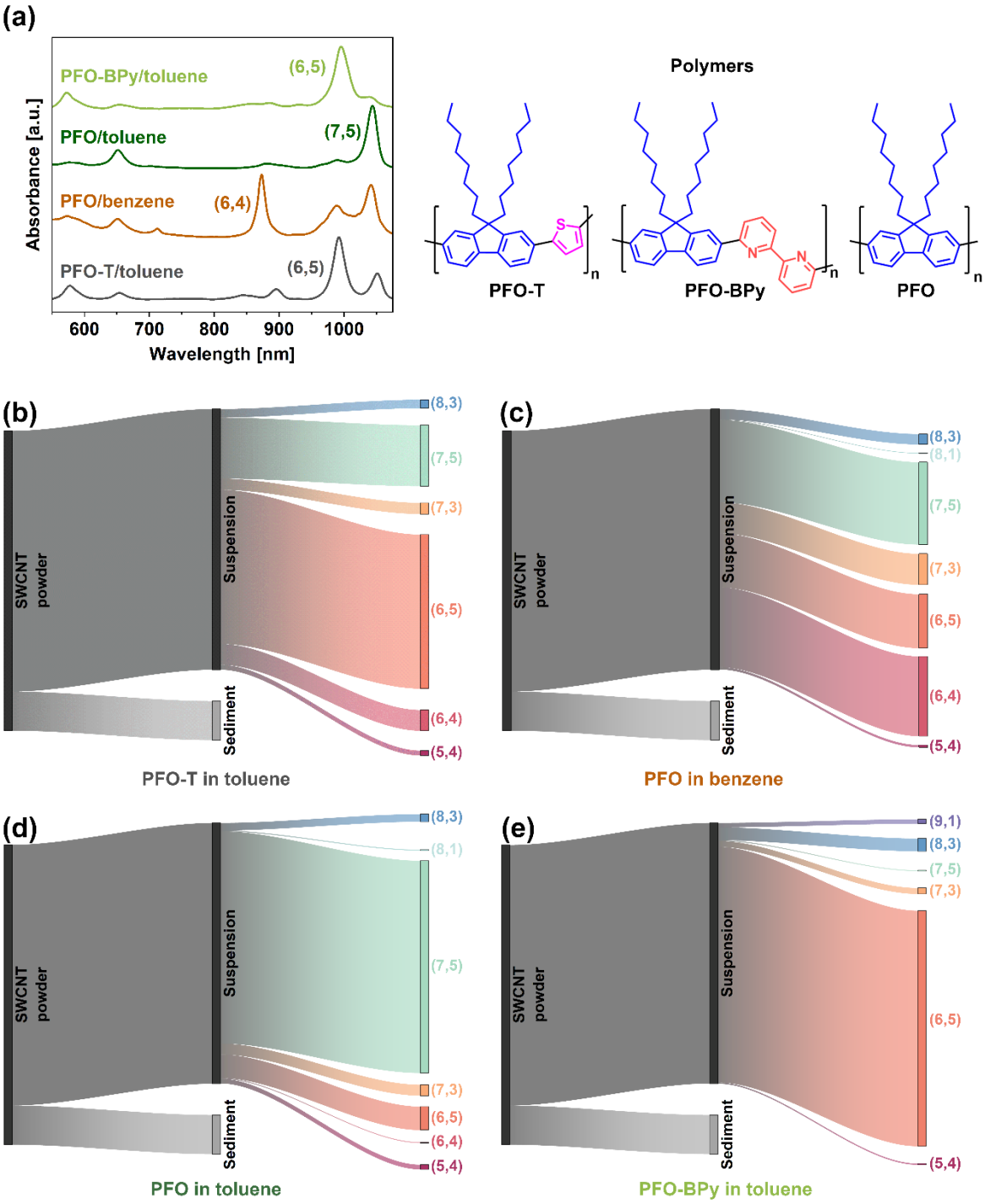

Figure S7 (a) Offset absorption spectra of (6,5)-enriched CoMoCAT SWCNTs individualized in various solvents by PFO, PFO-BPy, and PFO-T using the same conditions as before (structure of employed solvents and polymers is shown below). Composition of SWCNTs sorted by (b) PFO-T in toluene, (c) PFO in benzene, (d) PFO in toluene, and (e) PFO-BPy in toluene estimated using deconvoluted absorption data. The ratio of sediment to suspension presented in the diagram is for illustrative purposes only, as it depends on the polymer/SWCNT types and homogenization method.

7. Deconvolution of the composition of the supernatants obtained using non-selective and selective polymers

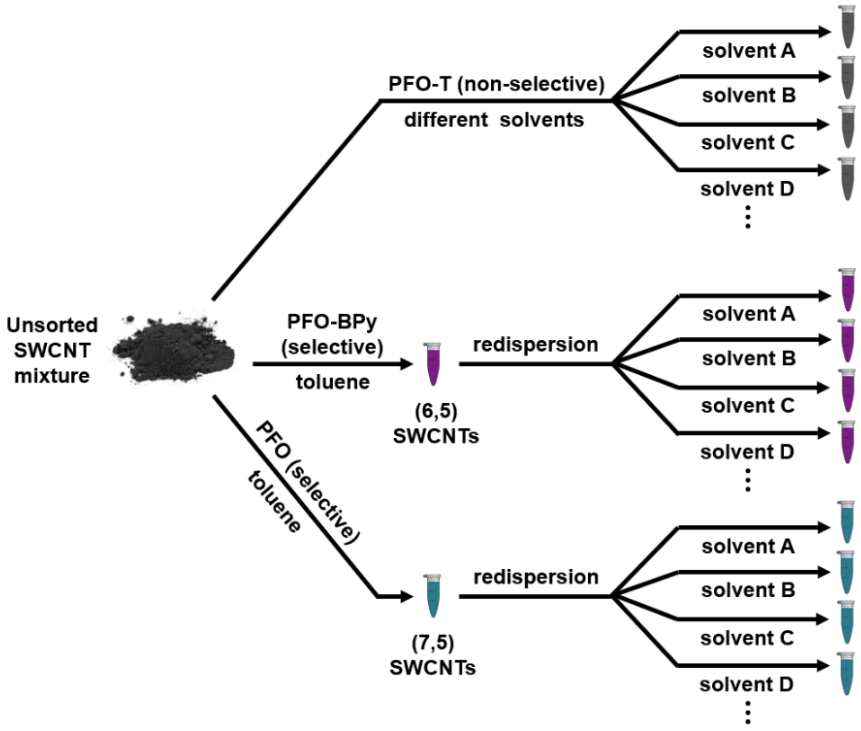

Figure S8 Modification of the approach used to determine solvatochromic shifts in SWCNTs suspended in various organic solvents.

8. Gauging the solvatochromic effect using SWCNTs isolated with selective polymers

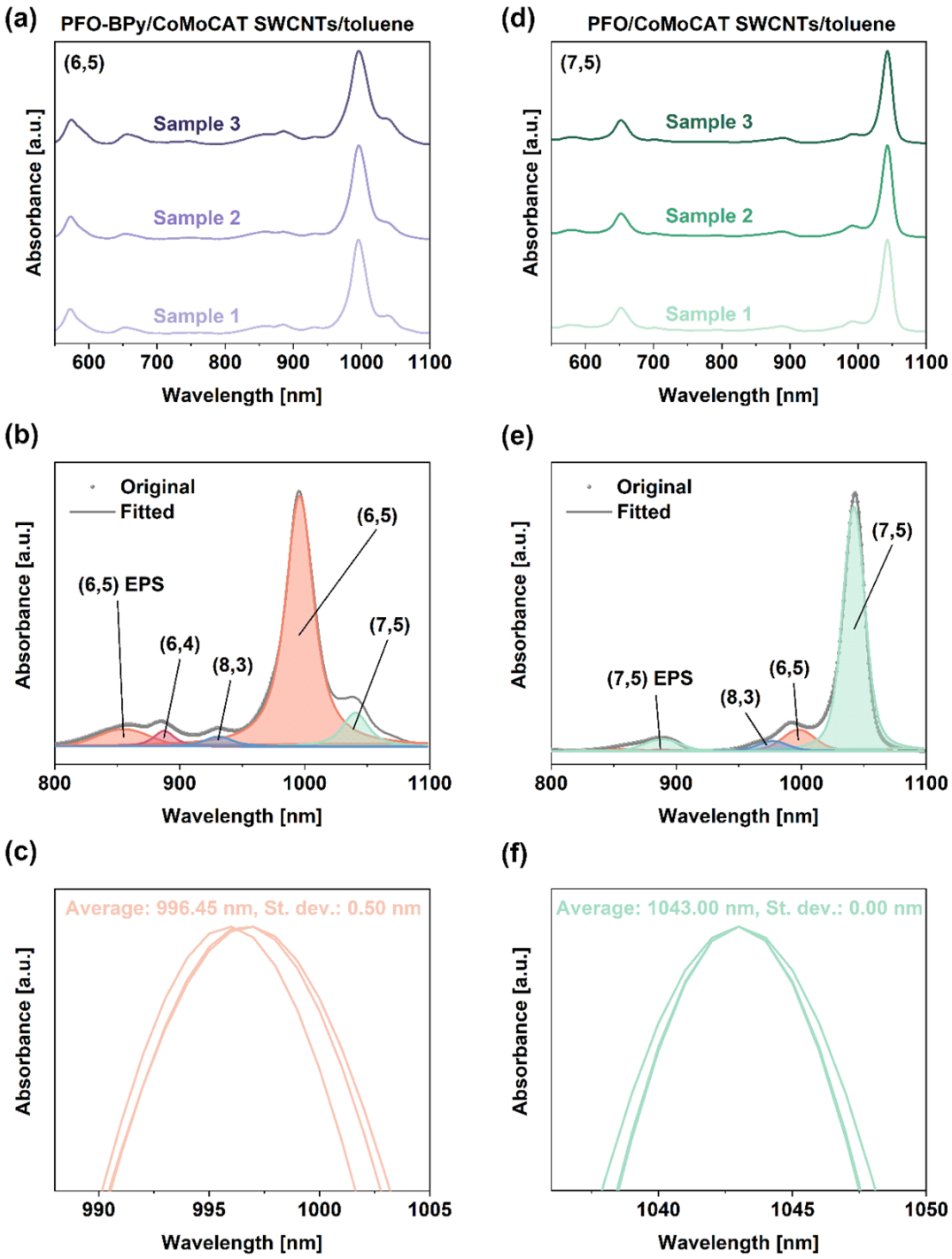

Figure S9 (a) Offset absorption spectra of three samples of (6,5)-enriched CoMoCAT SWCNTs solubilized in toluene using PFO-BPy to enrich the solution with (6,5) SWCNTs. (b) Deconvolution of the spectrum to resolve the contribution of individual chiralities. (c) Comparison of peak maxima positions of S_{11} optical transitions of (6,5) SWCNTs. (d) Offset absorption spectra of three samples of (6,5)-enriched CoMoCAT SWCNTs solubilized in toluene using PFO to enrich the solution with (7,5) SWCNTs. (e) Deconvolution of the spectrum to resolve the contribution of individual chiralities. (f) Comparison of peak maxima positions of S_{11} optical transitions of (7,5) SWCNTs.

We verified whether the observed shifts depended on the influence of the solvent exclusively or stemmed from the irreversible alteration of the polymer alignment on the SWCNT surface. To this end, after the measurement in THF, we decided to leave solutions from both conjugated polymers to evaporate, poured toluene back into them, and redispersed SWCNTs. The motivation was to check if the peak position returned to its original position, which would provide more understanding of the SWCNT-polymer-solvent interactions.

Fig. S10 shows the effect of this treatment on the shape of the absorption spectrum over the entire range, as well as (in magnification) the position of the peaks from the (6,5) and (7,5)-chiralities. Although the peak position first changed when moving from toluene to a solvent of higher polarity, in this case, THF, it returned to its original position on reverse switching. Some minor aberrations in the absorption spectra were concentrated around non-selectively suspended nanotubes, for which the intensity changed noticeably, especially in the case of PFO. This effect may indicate that the conformation of the investigated polymers on the non-selectively dispersed SWCNTs was particularly important, and small perturbations in the binding energy caused by the solvent replacement caused the precipitation of particular SWCNT types according to the scheme shown in Fig. S10e.

At this point, it is worth noting that all the listed elements, i.e., SWCNTs in suspension, those forming bundles and deposited on the bottom of the vessel, and the conjugated polymer present on the surface of the SWCNTs and in free form in solution, create a dynamic equilibrium [12]. This is shown by the fact that re-evaporation of the solvent and redispersion in toluene caused solubilization of previously precipitated SWCNTs. Also, the positions of the peaks coming from selectively suspended nanotubes, i.e., (6,5) for PFO-BPy and (7,5) for PFO, reverted to their original locations practically perfectly, which opened a new way to study the effects of solvatochromism in populations of nanocomposites formed by selective suspension by conjugated polymers.

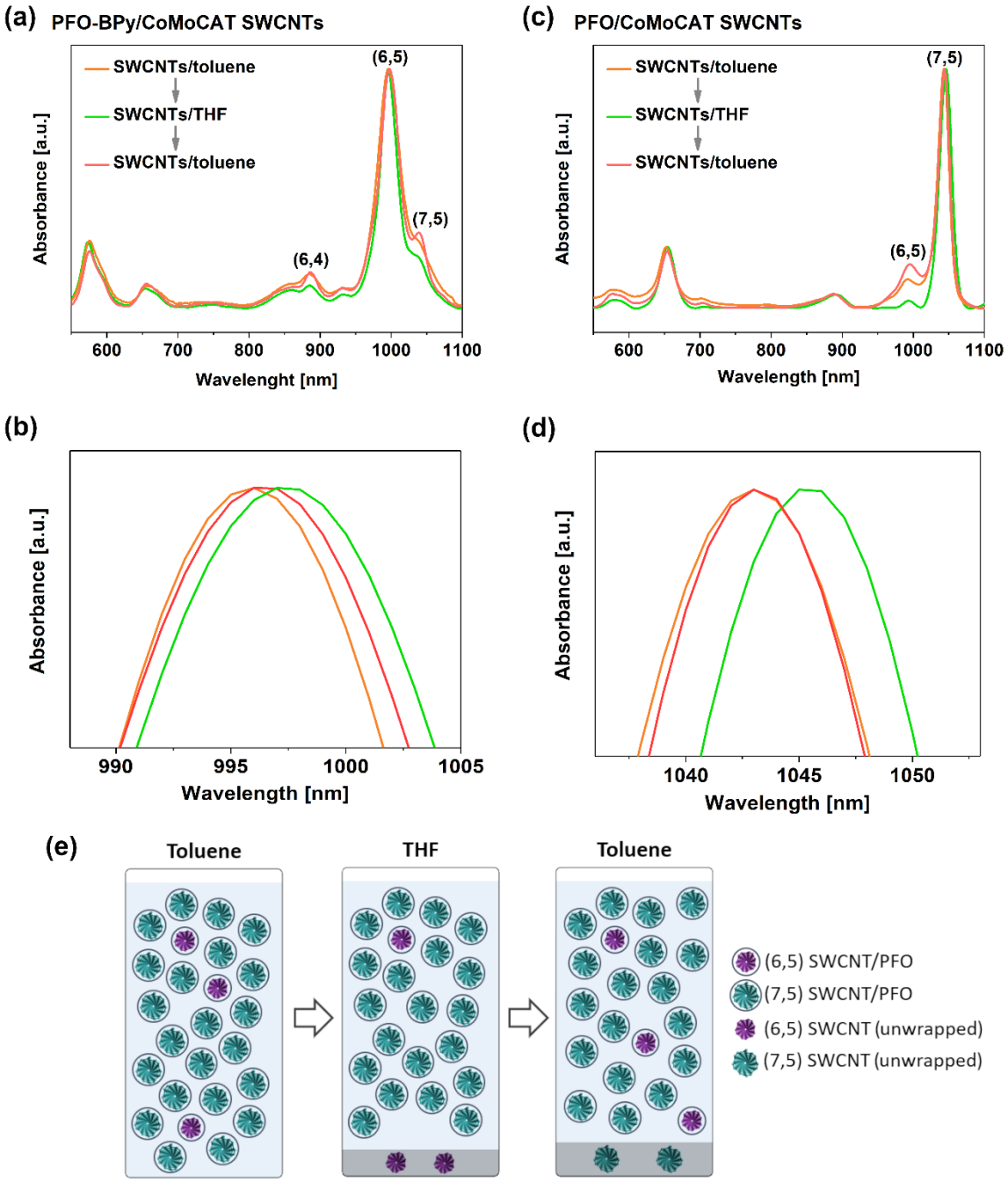

Figure S10 (a) Overlaid absorption spectra of (6,5)-enriched SWCNTs solubilized in toluene using PFO-BPy, evaporated and redispersed in THF, and evaporated and redispersed in toluene again. (b) Comparison of peak maxima positions of S_{11} optical transitions of (6,5) SWCNTs. (c) Overlaid absorption spectra of (7,5)-enriched SWCNTs solubilized in toluene using PFO, evaporated and redispersed in THF, and evaporated and redispersed in toluene again. (d) Comparison of peak maxima positions of S_{11} optical transitions of (7,5) SWCNTs. (e) Mechanism of redistribution of SWCNT composition.

9. Attempts to correlate properties of the solvent with optical characteristics of various SWCNTs separated in it

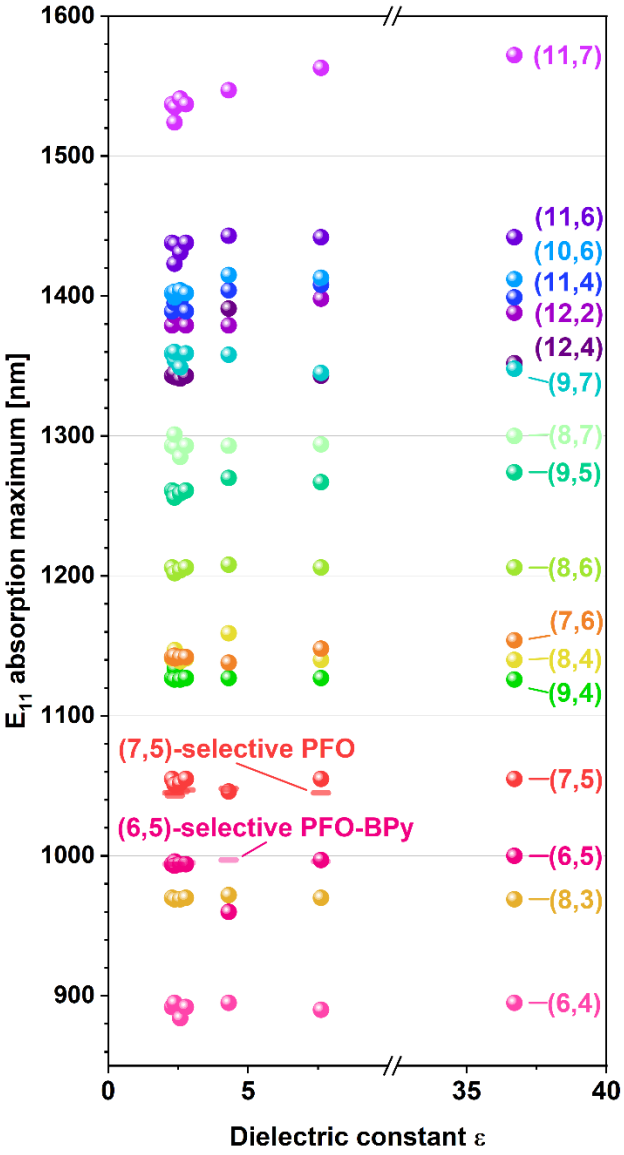

Figure S11 Overview of the E_{11} absorption peak maximum for different chiralities isolated by PFO-T, unless stated otherwise, as a function of the dielectric constant of examined solvents (see Table S1).

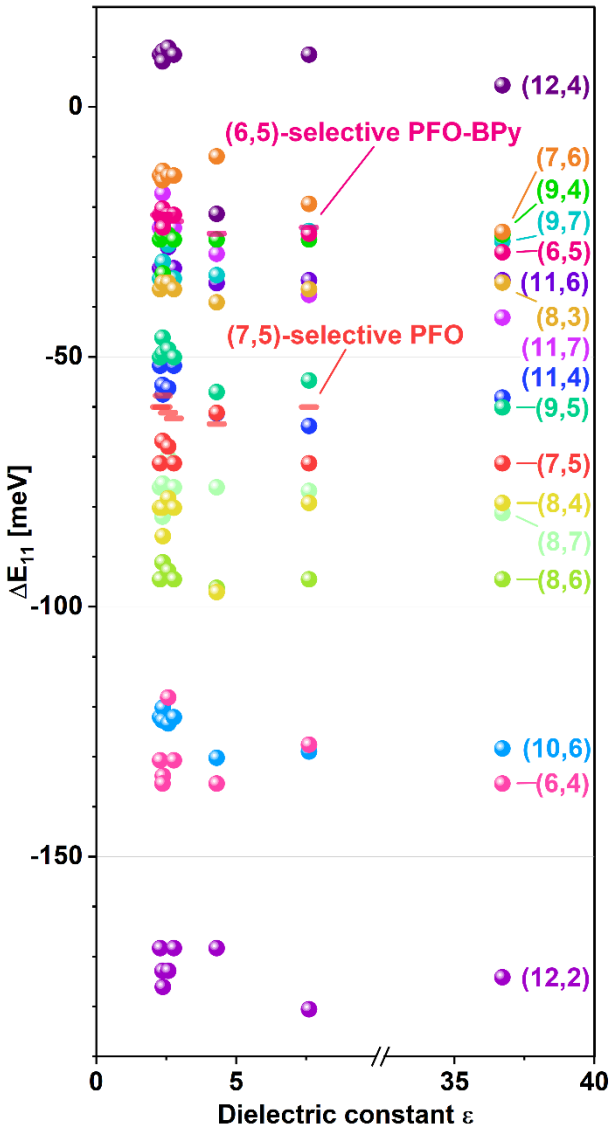

Figure S12 Overview of the spectral shift of absorption peak maximum ΔE_{11}, relative to the calculated E_{11} for SWCNTs in vacuum (E_{11VAC}), as a function of the dielectric constant of examined solvents (see Table S1). Data for chiralities isolated by PFO-T, unless stated otherwise.

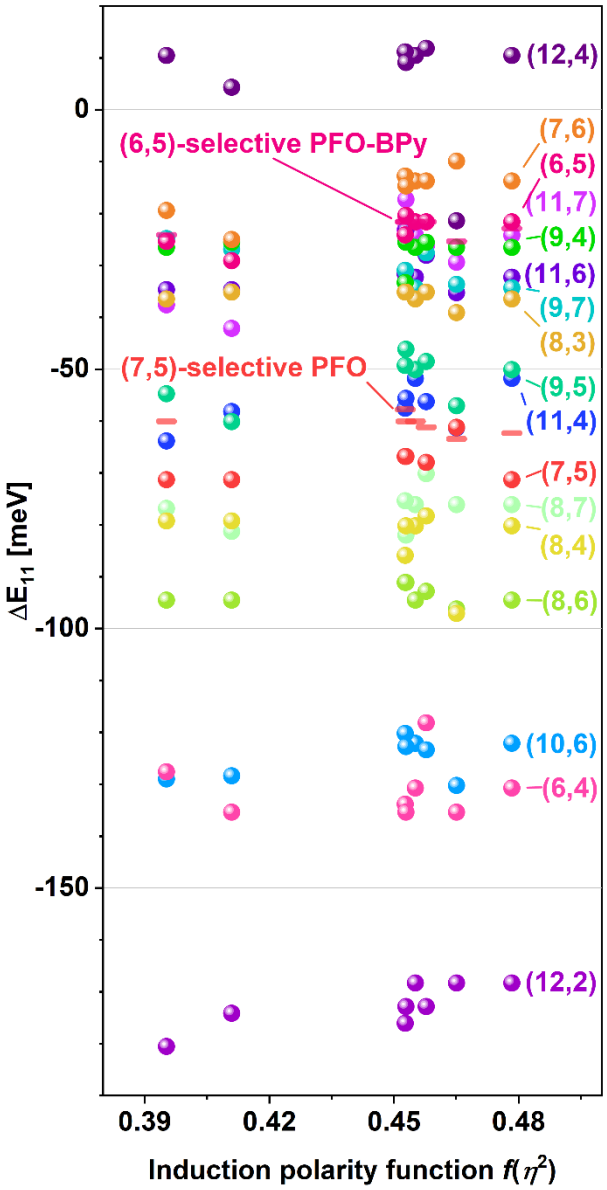

Figure S13 Overview of the spectral shift of absorption peak maximum ΔE_{11}, relative to the calculated E_{11} for SWCNTs in vacuum (E_{11VAC}), as a function of the induction polarity function of examined solvents (see Table S1). Data for chiralities isolated by PFO-T, unless stated otherwise.

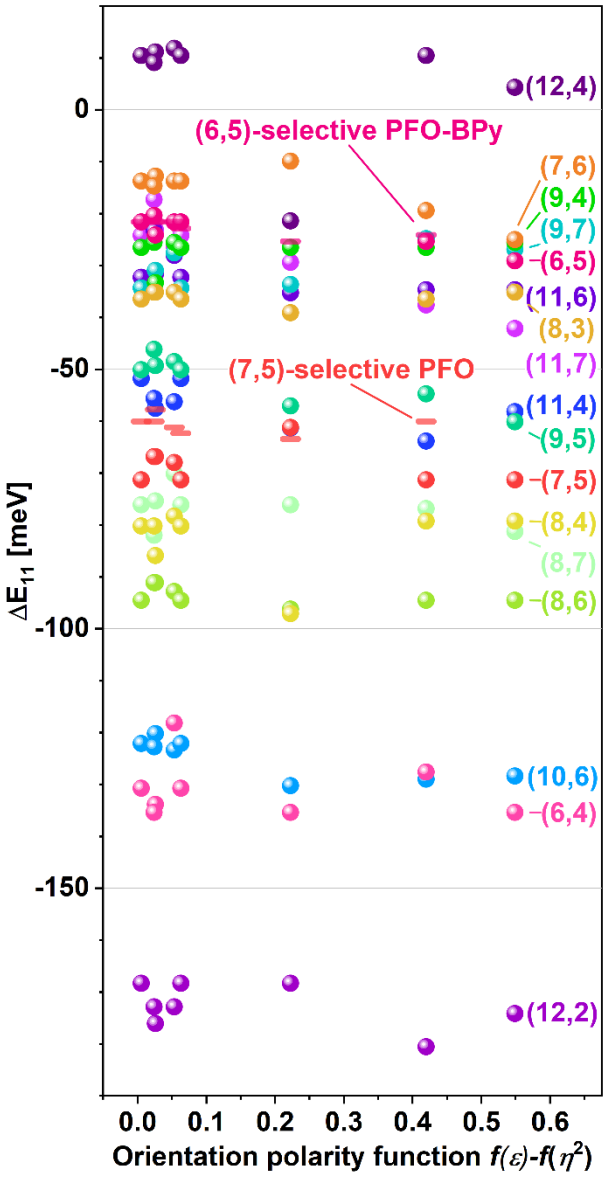

Figure S14 Overview of the spectral shift of absorption peak maximum ΔE_{11}, relative to the calculated E_{11} for SWCNTs in vacuum (E_{11VAC}), as a function of the orientation polarity function of examined solvents (see Table S1). Data for chiralities isolated by PFO-T, unless stated otherwise.

10. References

1 I. M. Smallwood, *Handbook of Organic Solvent Properties*, Elsevier, 2012.

2 C. Reichardt and T. Welton, *Solvents and Solvent Effects in Organic Chemistry*, Wiley-VCH Verlag GmbH & Co. KGaA, Weinheim, Germany, 2010.

3 C. Wohlfarth, *Static Dielectric Constants of Pure Liquids and Binary Liquid Mixtures*, Springer Berlin Heidelberg, Berlin, Heidelberg, 2015.

4 W. M. Haynes, *CRC Handbook of Chemistry and Physics*, CRC Press, 2014, vol. 268.

5 C. L. Yaws, *Thermophysical Properties of Chemicals and Hydrocarbons: Second Edition*, Elsevier, 2014.

6 R. Stenutz, Tables for Organic Chemistry, http://www.stenutz.eu/chem/, (accessed 14 November 2022).

7 S. Murov, Properties of Solvents Used in Organic Chemistry, http://murov.info/orgsolvents.htm, (accessed 14 November 2022).

8 Registered Substances Factsheets, https://echa.europa.eu/information-on-chemicals/registered-substances, (accessed 14 November 2022).

9 Flowline, Dielectric Constant, https://www.flowline.com/dielectric-constant/, (accessed 14 November 2022).

10 M. Pfohl, D. D. Tune, A. Graf, J. Zaumseil, R. Krupke and B. S. Flavel, *ACS Omega*, 2017, **2**, 1163–1171.

11 N. Nair, M. L. Usrey, W.-J. Kim, R. D. Braatz and M. S. Strano, *Anal. Chem.*, 2006, **78**, 7689–7696.

12 F. M. Chen, W. Zhang, M. Jia, L. Wei, X. F. Fan, J. L. Kuo, Y. Chen, M. B. Chan-Park, A. Xia and L. J. Li, *J. Phys. Chem. C*, 2009, **113**, 14946–14952.